International Journal of Solids and Structures 46 (2009) 3988–3998

Contents lists available at ScienceDirect

International Journal of Solids and Structures

journal homepage: www.elsevier.com/locate/ijsolstr

A numerical study on the rate sensitivity of cellular metals

Y.D. Liu, J.L. Yu *, Z.J. Zheng, J.R. Li

CAS Key Laboratory of Mechanical Behavior and Design of Materials, University of Science and Technology of China, Hefei, Anhui 230026, People's Republic of China

ARTICLE INFO

Article history:
Received 18 December 2008
Received in revised form 15 May 2009
Available online 6 August 2009

Keywords:
Voronoi honeycomb
Inertia
Strain hardening
Strain-rate hardening

ABSTRACT

Metallic foams have non-linear deformation behavior, which make them attractive in many applications. Many experimental researches on the dynamic behavior and rate sensitivity of cellular metals have been reported in the literature, but they contain conflicting, and sometimes confusing, conclusions on the strain-rate and inertia effect of cellular metals. In this paper, the dynamic crushing behavior of 2D Voronoi honeycomb is studied by finite element method. The influences of inertia, strain hardening and strain-rate hardening of metal matrix on the deformation mode and plateau stress of the honeycomb are investigated. Three deformation modes are found in different velocity ranges. According to the numerical results, it is found that the plateau stress increases significantly with the increase of impact velocity due to non-uniform deformation induced by inertia. The strain-hardening effect is slight in our numerical tests and the rate effect of the honeycomb is obviously weaker than that of the cell wall material.

1. Introduction

Cellular metals including foams and honeycombs are widely used as advanced structural components in many engineering applications due to their excellent physical, chemistry and mechanical properties. Potential applications of cellular metals include light weight cores for sandwich structures to increase the impact resistance, and improve the energy absorbing capacity. For such applications, understanding their mechanical behavior, particularly their response to dynamic loading is of strong importance to the engineering community, since strain rate and inertia may greatly affect the response. Much effort, including both experimental investigation and numerical analysis, has been made on the dynamic behavior of cellular metals, but there are some conflicting conclusions in the rate effect on their deformation behavior in the literature.

The most commonly used method for measuring the dynamic behavior of cellular metals is the split Hopkinson pressure bar (SHPB) technique. Tables 1 and 2 collected some experimental results in the literature on the strain-rate effect of open-cell and closed-cell aluminum foams, respectively. From these tables one can see that opposite conclusions exist for the rate sensitivity of both open-cell and closed-cell aluminum foams, related to their relative density, chemical composition, or method of process. Moreover, the closed-cell 6061 aluminum alloy foams produced by powder metallurgy with similar relative density show conflicting strain-rate sensitivity, as reported by Hall et al. (2000) and Zhao et al. (2005).

Numerical simulation are also widely applied to study the mechanical behavior and mechanisms of cellular metals. Many works have been done to reveal the mechanical properties of metallic honeycombs and foams under static loading. By using the finite element method, Voronoi honeycombs were employed (Silva et al., 1995; Zhu et al., 2001) to analyze the influence of the imperfection on the static crushing behavior. Tekoglu and Onck (2005) studied the influence of the ratio of specimen size to cell size on the effective mechanical properties of cellular materials by finite element analyses and the Cosserat continuum theory. Recently, they discussed the size effects in two-dimensional Voronoi foams in more detail (Tekoglu and Onck, 2008). Two continuum theories including the strain divergence theory and the micropolar theory were generalized to solve a range of basic boundary value problems, and the results were compared with numerical calculations based on a Voronoi representation of the cellular microstructure. It showed that the couple stress theory (a special case of the micropolar theory) and the strain divergence theory coincided well with the numerical calculations except for pure bending problem, but the micropolar theory with a small coupling factor could just predicted the response in uniaxial loading problem.

Generally speaking, the mechanisms of rate sensitivity of cellular metals may include the effects of intrinsic length scale of the material, the rate sensitivity of cell-wall material, the compression and flow of gas in cells, the micro-inertia effect, and other effects such as inertia and micro-structural morphology that may change the deformation mode of the material in dynamic cases. In the following we will first give a brief discussion on these effects.

* Corresponding author. Tel.: +86 551 360 0792; fax: +86 551 360 6459.
E-mail address: jlyu@ustc.edu.cn (J.L. Yu).

0020-7683/$ - see front matter © 2009 Elsevier Ltd. All rights reserved.
doi:10.1016/j.ijsolstr.2009.07.024

Table 1
Strain-rate effect of open-cell aluminum foams.

Brand	Material	Relative density	Processing method	Strain-rate effects	References
DUOCEL™	6061 Al	0.07	Investment casting	Insensitive	Dannemann and Lankford (2000)
DUOCEL™	6061 Al	0.07	Investment casting	Insensitive	Deshpande and Fleck (2000)
DUOCEL™	6061 Al	0.07	Investment casting	Insensitive	Lee et al. (2006)
M-PORE	Al, (Fe, Si)	0.05–0.08	Investment casting	Insensitive	Montanini (2005)
–	SG91A Al	0.03–0.06	Investment casting	Sensitive	Kanahashi et al. (2000)
–	Al–3Mg–8Si–1.2Fe	0.25–0.3	Infiltration	Insensitive	Wang et al. (2006)
–	Al	0.36–0.42	Infiltration	Sensitive	Han et al. (2005)

Table 2
Strain-rate effect of closed-cell aluminum foams.

Brand	Material	Relative density	Processing method	Strain-rate effects	References
ALPORAS™	Al, (Ca, Ti, Fe)	0.08–0.1	Batch casting	sensitive	Paul and Ramamutry (2000)
ALPORAS™	Al, (Ca, Ti, Fe)	0.106/0.155	Batch casting	sensitive	Mukai et al. (2006)
ALPORAS™	Al, (Ca, Ti, Fe)	0.074/ 0.15	Batch casting	sensitive	Dannemann and Lankford (2000)
ALULIGHT	Al, (Mn, Si)	0.16–0.31	Powder metallurgy	Insensitive	Deshpande and Fleck (2000)
SCHUNK	Al, (CaO_2)	0.07–0.28	Powder metallurgy	Sensitive	Montanini (2005)
IFAM™	6061 Al (Ti)	0.23	Powder metallurgy	Sensitive	Zhao et al. (2005)
–	6061 Al (Ti)	0.1–0.3	Powder metallurgy	Insensitive	Hall et al. (2000)
CYMAT	Al–SiC	0.09	Melt gas injection	Insensitive	Zhao et al. (2005)
CYMAT	Al–SiC	0.1–0.24	Melt gas injection	Insensitive	Montanini (2005)

Typical intrinsic length scale of metallic foams is in an order of 1 mm and the elastic wave speed in metals is of the order of 1000 m/s while the plastic wave speed in metals is of the order of 100 m/s. The wave speed in the solid part of the cellular metals should be in the same order. These data give a characteristic strain rate of $1 \times 10^5\ s^{-1}$. That is, only when the strain rate in the tests exceeds $1 \times 10^5\ s^{-1}$ metallic foams will show strain-rate effect due to the intrinsic length scale, which were obviously not the case for the SHPB tests.

It is known that pure aluminum is strain-rate sensitive and most aluminum alloys are strain-rate insensitive. So pure aluminum foams may also exhibit strain-rate sensitivity but the quantitative relation between the rate sensitivity of matrix material and that of the foam is not clear. It is perplexing that some of their foams exhibit opposite behavior, as shown in Tables 1 and 2.

According to Gibson and Ashby (1997), assuming an ideal gas under isothermal compression, the strength elevation by compression of the air in a closed-cell foam is

$$\Delta\sigma = \frac{p_0\varepsilon(1-2v_f)}{[1-\varepsilon(1-2v_f)-\rho^*/\rho_s]}, \tag{1}$$

where p_0 is the atmospheric air pressure, v_f and ρ^*/ρ_s are the Poisson's ratio and the relative density of the foam, respectively. A similar calculation assuming adiabatic compression gives (Deshpande and Fleck, 2000)

$$\Delta\sigma = p_0\left[\left(\frac{1-\rho^*/\rho_s}{1-\varepsilon(1-2v_f)-\rho^*/\rho_s}\right)^{\gamma}-1\right], \tag{2}$$

where γ is the ratio of the specific heat capacities, with $\gamma = 1.4$ for air. The increase of the collapse stress in dynamic cases should not exceed the difference calculated by Eqs. (1) and (2) in the absence of strain-rate or inertial effects. For typical values of aluminum foams, this increase is negligible in comparison with the collapse stress itself, except for foams with very low relative density. For open-cell aluminum foams, the increase of the collapse stress in dynamic cases should not exceed the value calculated by Eq. (2), which is also negligible when the relative density of the foam is not very low. So the strain-rate sensitivity found in some aluminum foams cannot be attributed to the effect of gas compression and flow.

Micro-inertia effect was used by many authors to explain their experimental results where a significant elevation of collapse stress was found in the dynamic response of aluminum foams. Under dynamic conditions, micro-inertia of the individual cells can affect the deformation of cellular structures as it tends to suppress the more compliant buckling modes and thus to increase the crushing stress. However, as pointed out by Deshpande and Fleck (2000), metallic foams behave as Type I structures and deform predominantly by the bending of cell edges. It is thus expected that micro-inertia effects play little role in enhancing the dynamic crush strengths of metallic foams.

Recently, Tan et al. (2005a) carried out an extensive experimental study on the crushing behavior of closed-cell Hydro/Cymat aluminum foam. They found that the plastic collapse stress increases with the impact velocity and micro-inertial effects are responsible for the enhancement of the dynamic plastic collapse stress at the sub-critical velocities. When the impact velocity exceeds a critical value the deformation of the foam is of "shock-type" due to inertia effects. Below the critical velocity, the dynamic plateau stresses are insensitive to the impact velocity. Meanwhile, a one-dimensional "steady-shock" model based on a rate-independent, rigid, perfectly plastic, locking (R–P–P–L) idealization of the quasi-static stress–strain curves for aluminum foams was proposed (Tan et al., 2005b) to provide a first-order understanding of the dynamic compaction process.

Regular honeycombs (Ruan et al., 2003) and 2D Voronoi honeycombs (Zheng et al., 2005) were used to investigate the mechanism of dynamic crushing of cellular metals numerically. The influences of cell wall thickness and the irregularity of honeycombs, as well as the impact velocity, on the deformation mode and the plateau stress were investigated. Lately, Zou et al. (2009) also studied the in-plane dynamic crushing behavior of 2D hexagonal-cell honeycombs to investigate the features of the crushing front and to examine the assumptions employed in a one-dimensional shock theory (Tan et al., 2005b). It has been shown that there exists a zone where the material "particle velocity", "stress" and "strain" are discontinuous when the crushing velocity exceeds a critical value and that the one-dimensional shock theory tends to overestimate slightly the crushing stress and energy absorbed. In this paper, considering the structural features of hexagonal-cell honey-

comb, a relatively precise definition of the "particle" velocity, local engineering strain and engineering stress is introduced to illustrate the plateau stress and the total dissipated energy. It is very useful and explicit to know the engineering stress and strain field in the whole honeycomb along the loading direction. Ma et al. (2009) studied the dynamic behavior of metallic cellular materials. They developed a mesoscale numerical model based on Voronoi tessellation to investigate the loading rate effect on the crushing stress of cellular materials. A continuum model was introduced to explain the reason for the argument on the rate dependence of cellular materials and its results were in coincidence with the current numerical results. They also discussed the influences of the impact velocity, specimen size, inertia and rate dependence of the base materials on the crushing stress, and found that the crushing stress at the stationary side was insensitive to loading rate unless that the base material had strong rate dependency, but they did not give more explanations.

Although experimental study is the essential means to obtain the mechanical behavior of materials, there are some limitations associated to dynamic tests of foam materials. As pointed out by Deshpande and Fleck (2000), metallic foams are highly heterogeneous imperfect materials with a dispersion strength of the order of 20%. Microscopically there are many morphological defects. So comparison among specimens is not easy. More over, when loading at high strain rates, the homogeneity of deformation required by SHPB cannot be guaranteed. Besides, accurate measurement of strain distribution is nearly impossible. All these facts make experimental studies very difficult, especially when high strain rate is concerned. As experienced by many researchers, the repeatability of tests is limited and dispersion of strength data may cover up the rate sensitivity. Due to the high porosity and low density, uniformity of stress and strain required by the SHPB tests may not be satisfied and the accuracy in dynamic experiments is questionable. Finally, we cannot solely change the inertia of specimens to study its effect.

Contrary to experimental approach, in numerical simulation we can focus our attention on influence of a single parameter. An identical sample ("specimen") can be used in numerical simulation under different conditions and the density of cell wall material may be artificially changed to explore the inertia effect.

In this paper, in order to clarify the inconsistencies in the literature mentioned above, we employ 2D Voronoi honeycomb in our numerical simulations (or, "numerical experiments"). The density and plastic hardening properties of the cell wall material are factitiously changed to investigate the effects of inertia, strain hardening and strain-rate hardening on the crushing behavior of Voronoi honeycombs.

2. Methods and materials

2.1. 2D random Voronoi technique

The 2D random Voronoi technique presented in literatures (Zhu et al., 2001; Zheng et al., 2005) was employed to generate 2D Voronoi honeycombs. N nuclei are generated in a square area A_0 by the principle that the distance between any two points is not less than a given distance δ. Then these nuclei are copied to the surrounding neighboring areas by translation. Use the set of these $9N$ nuclei to construct the Delaunay triangulation and even the Voronoi diagram. The condition satisfied by a Voronoi cell is that it contains all points that are closer to its data point than any other data point in the set. Finally, the part of the Voronoi diagram out of the square area A_0 is deleted to reserve a periodic Voronoi structure. The character of this 2D random Voronoi technique is illustrated in Fig. 1a. The irregularity of a Voronoi honeycomb with N cells in a square area A_0 is defined as (Zhu et al., 2001)

$$k = 1 - \delta \Big/ \sqrt{2A_0/\sqrt{3}N}. \tag{3}$$

The relative density of a honeycomb is specified by

$$\bar{\rho} = \rho^*/\rho_s = \frac{1}{A_0}\sum h_i l_i, \tag{4}$$

where ρ^* is the density of honeycomb, ρ_s the density of its cell wall material, l_i the ith cell wall length and h_i the corresponding thickness (Zheng et al., 2005).

2.2. Finite element models

Fig. 1b shows a sample of Voronoi honeycomb constructed in an area of $100 \times 100\ \text{mm}^2$ with 200 nuclei. The irregularity of the Voronoi honeycomb samples is taken to be 0.45 and the number of samples is five in our finite element models. The cell wall thickness is identical in all cells and in the samples. Three values of thickness, i.e., 0.26, 0.36 and 0.48 mm, are investigated, corresponding to relative densities of approximately 0.073, 0.1 and 0.135, respectively. More values of relative densities are chosen to study the relationship between the relative density and the plateau stress. Meanwhile, the thickness (H) in the out-of-plane direction is 1 mm here. In these finite element models, cell walls shorter than the thickness were eliminated and the associated cell corners merged together to ensure the process of the FEA. Each edge of the cell wall is divided into a few shell elements of type S4R (a 4-node quadrilateral shell element with reduced integration) with five integration points. The number of shell elements depends on the

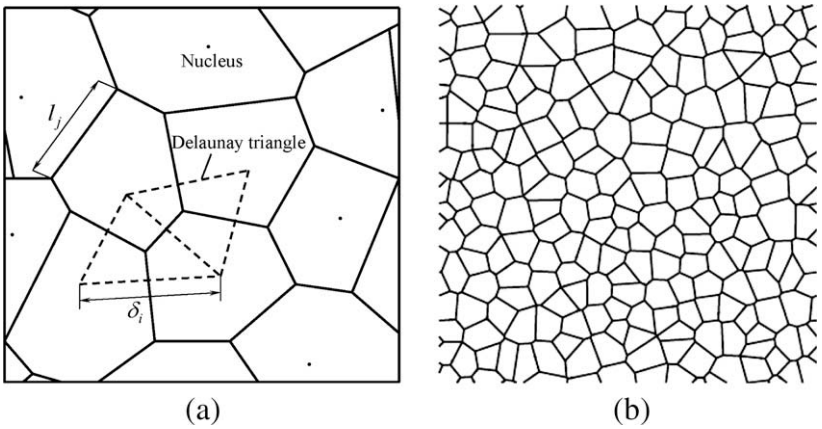

Fig. 1. 2D random Voronoi technique: (a) formation of the grid, (b) a sample with $k = 0.45$.

edge length, with an average of six and the mean element length of about 0.8 mm. Each model consists of about 6700 shell elements. For every Voronoi honeycomb, self-contact is specified between all faces of cells that may contact in the process of crushing and an outside layer is added to carry out this self-contact. Thickness of the outside layer is taken as 1/10 of the cell wall thickness. Finally, the honeycomb is sandwiched between two rigid platens, their contacting edges can slip on both interfaces with slight friction and the friction coefficient is assumed as 0.02. In the simulation, the left platen is stationary and the right platen moves leftward with a constant velocity, and the top and bottom edges are free. Meanwhile, the 3rd degree of freedom (out-of-plane direction) is constrained during the crashing process. Thus, the nominal engineering stress, strain and strain rate are defined as

$$\sigma = F/A, \quad \varepsilon = S/L, \quad \dot{\varepsilon} = V_i/L, \tag{5}$$

where F is the contact reaction force on the reference points of the two rigid platens, $A = L \times H$ the nominal contact area, L the initial length of the specimen ($L = 100$ mm in this paper), S is the distance of the left rigid platen and V_i is the corresponding impact velocity. In fact, the nominal strain and the nominal strain-rate are suitable only for the case of homogenous deformation. When the global deformation localization takes place, these definitions lose their physical meanings since their values are size dependent. Use them in the latter condition is only for the purpose of comparison, as ε and $\dot{\varepsilon}$ could reflect the averaged deformation and deformation rate of the crashed honeycomb, respectively.

In this paper, ABAQUS/EXPLICIT is employed to analyze the uniaxial compression behavior of Voronoi honeycombs under different impact velocities. Samples are compressed in one direction under different velocities and the other direction is free.

In order to reveal the influence of cell wall materials on the crushing behavior, we take three kinds of cell wall materials into account. The first one is elastic–perfectly plastic with Young's modulus, yield stress and Poisson's ratio being 66 GPa, 175 MPa and 0.3, respectively. The second one is elastic–plastic material with linear strain-hardening. The third one is elastic–perfectly plastic material with strain-rate hardening. The stress–strain relations in the plastic stage for the last two materials are defined as

$$\sigma = \sigma_y + B\varepsilon_p \tag{6}$$

and

$$\sigma = \sigma_y[1 + C\ln(\dot{\varepsilon}_p/\dot{\varepsilon}_0)] \tag{7}$$

respectively, where ε_p is equivalent plastic strain, σ_y the yield strength of cell wall material, $\dot{\varepsilon}_p/\dot{\varepsilon}_0$ the relative equivalent strain rate, B and C are material constants (Johnson and Cook, 1983). Here we take $B = 175$ MPa and $\dot{\varepsilon}_0 = 0.1$. Two levels of the strain-rate sensitivity are considered with $C = 0.05$ and $C = 0.4343$, which will be referred to Rate Sensitive Material 1 (RS1) and Rate Sensitive Material 2 (RS2), respectively, in the following.

For the purpose of quantitative comparison and analysis, the plateau stress is specified by

$$\sigma_p = \frac{1}{\varepsilon_D - \varepsilon_y}\int_{\varepsilon_y}^{\varepsilon_D} \sigma\, d\varepsilon, \tag{8}$$

where the densification strain ε_D is defined as (Tan et al., 2005a)

$$\frac{d}{dt}\left[\frac{1}{\sigma}\int_0^{\varepsilon}\sigma\, d\varepsilon\right]\Big|_{\varepsilon=\varepsilon_D} = 0, \tag{9}$$

and ε_y is the yield strain, which is taken as 0.02 in this study.

3. Results

3.1. Deformation modes and the critical velocity of mode transition

Zheng et al. (2005) have found that the deformation of Voronoi honeycombs under dynamic compression is complicated but it can be catalogued into three modes. A Quasi-static Homogeneous Mode occurs under low impact velocities, in which the crush bands are randomly located and the deformation is macroscopically homogeneous. If the impact velocity is very high, a Shock or Dynamic Mode occurs and cells crush sequentially in a planar manner from the impact end. A Transition Mode occurs in between, in which the crush bends are more concentrated near the impact end than the support end.

In the present study, it is found that when the density of the elastic–perfectly plastic material is 2.7×10^3 kg/m^3 and the relative density is 0.1, the critical velocities between the corresponding modes are about 20 and 80 m/s, respectively. The definition of the critical velocities will be given later. For two different relative densities (0.073 and 0.135), when we keep the total mass of the honeycombs identical by changing the density of the cell wall material, the critical velocities between the corresponding modes increase a little (less than 10%) as the relative density increases. Likewise, the critical velocities of other two cell wall materials grow a bit larger (about 10%) than these of the elastic–perfectly plastic material. Three deformation modes under impact velocities of 10, 60 and 120 m/s, respectively, are shown in Fig. 2. The corresponding nominal stress–strain curves on the impact surface and the support surface are shown in Fig. 3. It is found that the plateau stresses calculated on the support surface for different modes are almost the same.

In Homogeneous Mode, the nominal stress–strain curves on the impact surface and the support surface are approximately the same and the plateau stresses calculated on the two surfaces are nearly equal, indicating an early achievement of internal force equilibrium. To describe the uniformity of macroscopic deformation, we introduce a uniformity coefficient defined by

$$\varphi = \frac{\sigma^s_{\mathrm{pl}}}{\sigma^i_{\mathrm{pl}}}, \tag{10}$$

where σ^i_{pl} is the plateau stress on the impact surface and σ^s_{pl} the plateau stress on the support surface. The plateau stresses on the two surfaces and the uniformity coefficient under different impact velocities of the elastic–perfectly plastic material are shown in Fig. 4a and b, respectively. If we take the uniformity coefficient of 90% as a critical value, then the critical impact velocity of mode transition between Homogeneous Mode and Transition Mode is almost 20 m/s. In this paper, the critical velocity for mode transition between the Homogeneous Mode and Transition Mode is defined when the uniformity coefficient is reduced to 90%.

The critical velocity between the Transition Mode and the Dynamic Mode is considered in Reid's R–P–P–L model (Tan et al., 2005b; Li and Reid, 2006). It is hard to give an accurate definition of the critical velocity. Here, we define it as follows. When the deformed band oriented perpendicular to the loading direction and only a single layer is in the collapse process while the other layers behind it have already been densified, the deformation mode is regarded as Shock Mode. The corresponding minimum impact velocity is taken as the critical velocity between the Transition Mode and the Shock Mode.

It transpires that the critical velocities of mode transition are nearly the same for cell wall materials with or without strain or strain-rate hardening, except for material RS2 with very strong strain-rate sensitivity, which has higher critical velocities. Generally speaking, strain and strain-rate hardening effect can contrib-

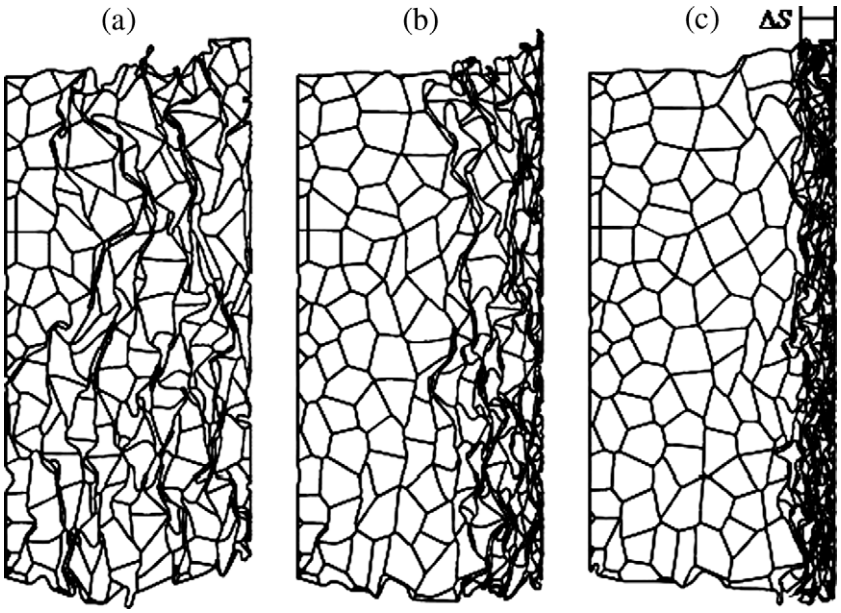

Fig. 2. Three deformation modes: (a) Homogeneous Mode, (b) Transition Mode and (c) Shock Mode.

ute positively to the uniformity of the deformation, so the critical velocities for material RS2 are a little higher. But for strain hardening material RS1, this effect may be not enough to cause a significant change.

Reid and Peng (1997) found that the "shock-enhanced" plateau stress in wood is simply given by

$$\sigma = \sigma_0 + Av^2. \tag{11}$$

It is found that this relation is also valid for regular honeycombs (Harrigan et al., 1999; Ruan et al., 2003), irregular honeycombs (Li et al., 2007) and foams (Tan et al., 2005a). In our numerical simulation, it is also found that, when the honeycombs are deformed in Transition Mode or Shock Mode, Eq. (11) is valid.

3.2. Inertia effect

Four values of the density of cell wall material, i.e., 2.7×10^3, 0.9×10^3, 0.3×10^3 and 0.1×10^3 kg/m^3, are chosen artificially to explore the effect of inertia and elastic–perfectly plastic material property is assigned. Simulations are performed for Voronoi honeycombs with identical sample pattern and the same relative density $\bar{\rho} = 0.1$ (i.e., the cell wall thickness is fixed), but compressed under different impact velocities in Homogeneous Mode. It is found that the calculated nominal stress–strain curves under different impact velocities remain almost identical, regardless of different densities of cell wall material, as shown in Fig. 5. It is evident that the inertia effect is negligible when the deformations of the honeycombs are macroscopically homogeneous.

Fig. 6 shows the nominal stress–strain curves of Voronoi honeycombs with the same cell wall material density but different relative density at $v = 1$ m/s. This figure clearly indicate that the plateau stress mainly depends on the relative density (the cell wall thickness), in agreement with experimental results reported in the literature.

The plateau stresses on the impact surface and support surface under different velocities for the cell wall material density of 2.7×10^3 kg/m^3 are shown in Figs. 7a and b, where I, II and III denote roughly the regions of Homogeneous, Transitional and Shock Modes, respectively. Note that the division of three regions is just to make the discussion easier since the differences of the transition velocities for different relative densities are small. It does not mean that the transition velocities are independent of the relative density. Also, it is not applied to another curve with the cell wall material density of 0.3×10^3 kg/m^3, which will be discussed later. It is found that, due to the inertia effect, the plateau stress on the impact surface in the Transitional Mode and Shock Mode increases rapidly with the increase of impact velocity. This is in agreement with the experimental results on square tubes (Zhao and Abdennadher, 2004) and wood (Reid and Peng, 1997). However, the plateau stress on the support surface exhibits little velocity dependence. This is in accordance with the inhomogeneous deformation of the sample. The enhancement of the plateau stress on the impact surface can be explained as follows. The macroscopic strain along the impact direction is not uniform. The layer near the impact surface has the maximum macroscopic strain and the stress and strain there are located in the densification portion of the nominal stress–strain curve. The difference in macroscopic strain distribution between the two modes is that in Shock Mode it is shock-like while in Transition Mode it changes gradually.

For comparison, the plateau stresses on the impact surface under different impact velocities for the cell wall material density of 0.3×10^3 kg/m^3 is also shown in Fig. 7a. It transpires that, with the reduction of inertia, the force equilibrium and uniform deformation become much easier and the critical velocities of mode transition increase dramatically. It is obvious that inertia effect is very important for the deformation of honeycombs under high impact velocity.

From Fig. 7b, it can be found that there is a drop in the stress on the support surface with increasing velocity during the Transition Mode. This is in agreement with the results of an experimental study on wood by Harrigan et al. (2005). This phenomenon is mainly due to the character of stress wave propagation in cellular materials. Unlike solid materials, when a stress wave propagates in a cellular material, it will disperse and attenuate. If the specimen length is long enough, at first only elastic part of the wave will reach the support surface, regardless whether the impact velocity is high or low. For a specimen with finite length, the stress on the support surface will further increase due to wave reflection and interaction, which mainly depends on the duration of loading

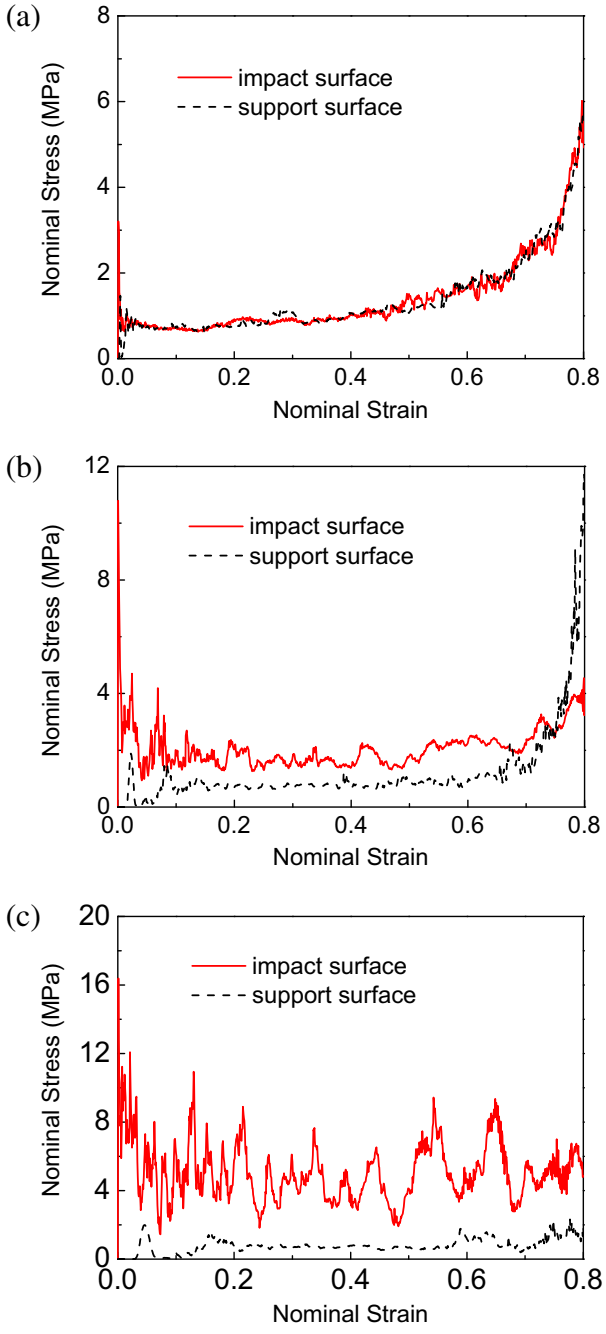

Fig. 3. Nominal stress–strain curves on the impact surface and support surface under (a) Homogeneous Mode, (b) Transition Mode and (c) Shock Mode.

time. Under a low impact velocity, the stress wave can propagate forth and back many times between the impact surface and the support surface, so the stress on the support surface increases until an equilibrium state is reached. On the other hand, under high impact velocities, the material near the impact surface soon became densified and the duration of response is short. So with increasing impact velocity, the interaction time becomes short and the stress on the support surface increases less.

3.3. Influence of the cell-wall material properties

To investigate the effect of cell-wall material properties on the crushing behavior, we select the linear strain-hardening and strain-rate hardening elastic–plastic materials to study the responses of the Voronoi honeycombs under various velocities. The density of cell wall material is 2.7×10^3 kg/m^3 and the relative density is $\bar{\rho} = 0.1$. The calculated plateau stresses with their mean square deviations under different impact velocities and a comparison of plateau stress on the impact surface of honeycomb samples

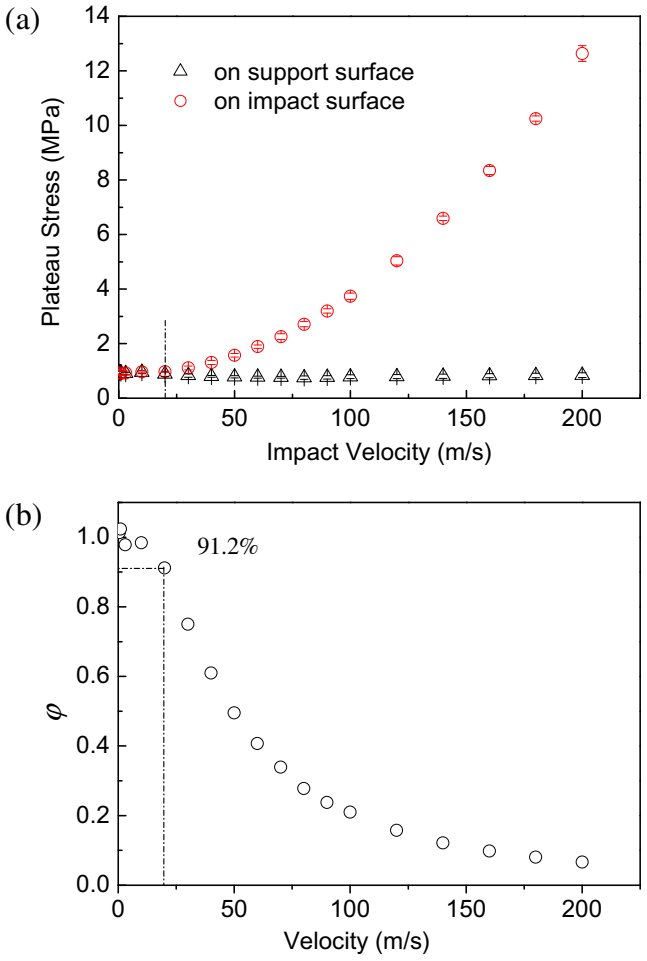

Fig. 4. Variations in (a) plateau stress on the impact surface and support surface and (b) the uniformity coefficient with impact velocity.

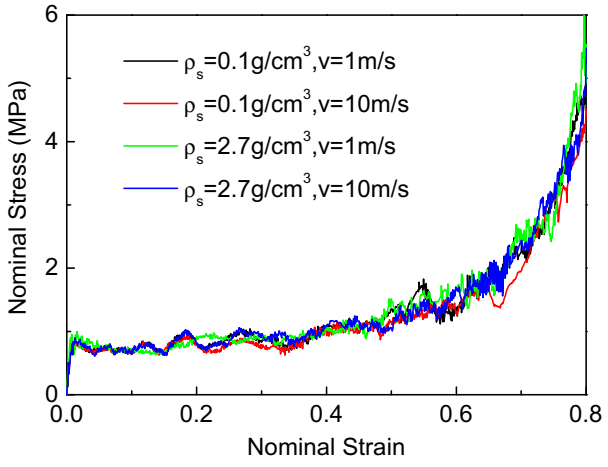

Fig. 5. Stress–strain curves of Voronoi honeycombs with relative density of $\bar{\rho} = 0.1$ under Homogeneous Mode.

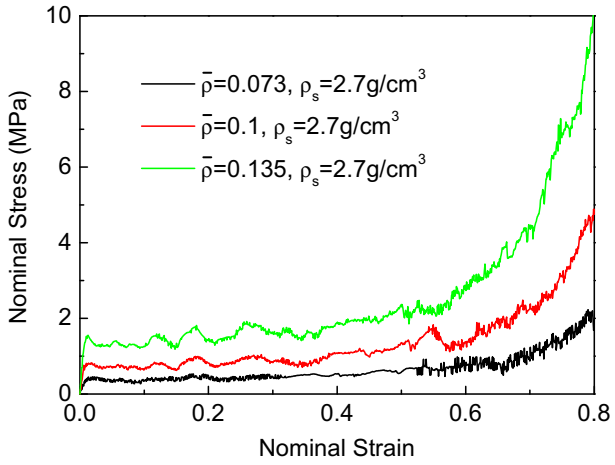

Fig. 6. Stress-strain curves of Voronoi honeycombs under Homogeneous Mode under impact velocity $v = 1$ m/s.

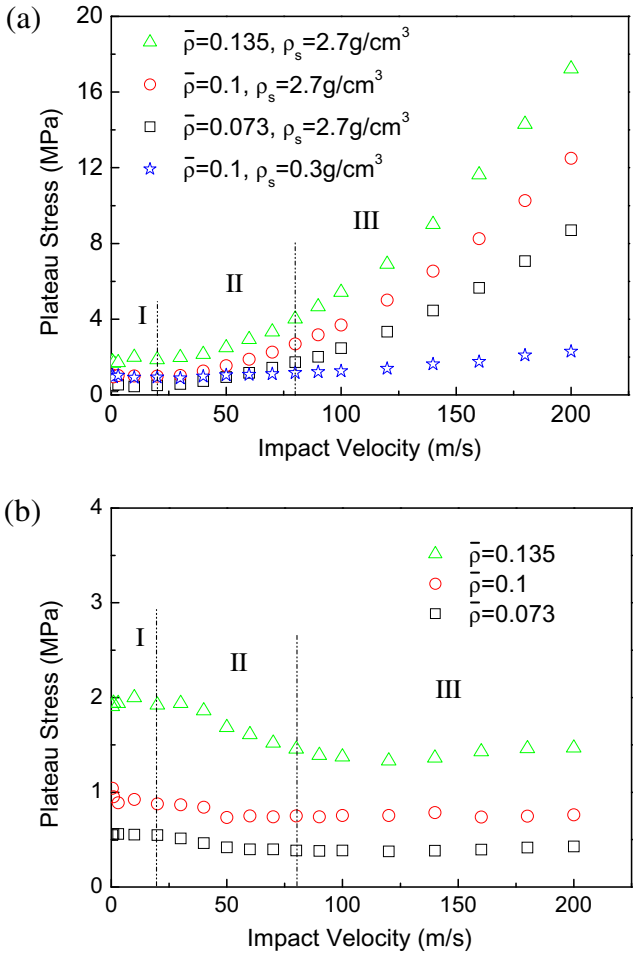

Fig. 7. Variations in the plateau stress (a) on the impact surface and (b) on the support surface with impact velocity for honeycombs with different relative densities.

made of elastic–perfectly plastic materials RS1 and RS2 are shown in Fig. 8. It is found that the increase in the plateau stress due to the strain-rate sensitivity of cell wall material is almost independent of the impact velocity.

In comparison with the elastic–perfectly plastic material, the relative increase in the plateau stress caused by the linear strain-hardening effect can be specified by

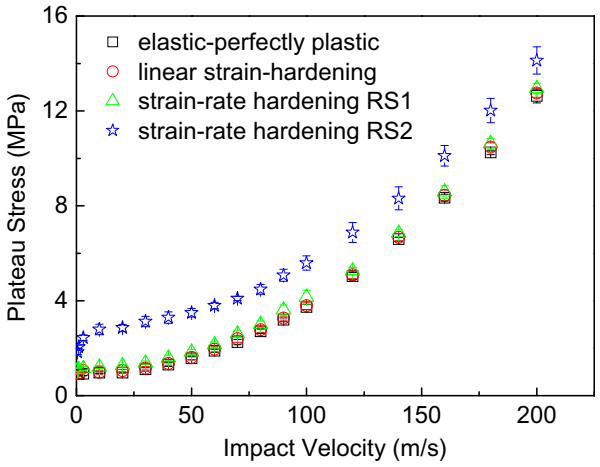

Fig. 8. Comparison of the plateau stresses of honeycombs made of different cell-wall materials under different impact velocities.

$$\lambda = (\sigma_1 - \sigma_0)/\sigma_0, \tag{12}$$

where σ_0 and σ_1 are the plateau stresses of the elastic–perfectly plastic material and the strain-hardening material, respectively. Note that the relative increase in the flow stress of the solid material is proportional to the plastic strain.

Similarly, the relative increase in the plateau stress caused by the strain-rate hardening effect, compared to elastic–perfectly plastic material, can be defined as

$$\eta_1 = (\sigma_2 - \sigma_0)/\sigma_0, \tag{13}$$

where σ_2 is the plateau stress of the strain-rate hardening material. According to Eq. (7), the relative increase in the flow stress of the solid material is described by

$$\eta_2 = (\sigma - \sigma_y)/\sigma_y = C\ln(\dot{\varepsilon}_p/\dot{\varepsilon}_0). \tag{14}$$

The variation of the averaged relative increase in the plateau stress on the impact surface of five random samples and their mean square deviations with the impact velocity for honeycombs made of strain-hardening material is shown in Fig. 9. It is found that λ takes a small value over the whole range of the impact velocities studied, so the strain-hardening of cell wall material has min-

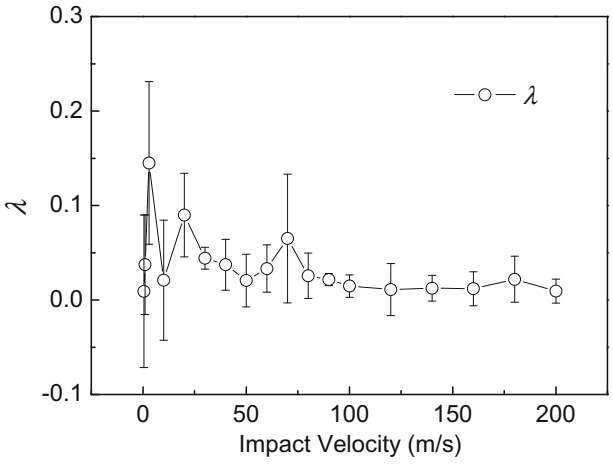

Fig. 9. Relative increase in the plateau stress of honeycombs made of strain-hardening material under different impact velocities.

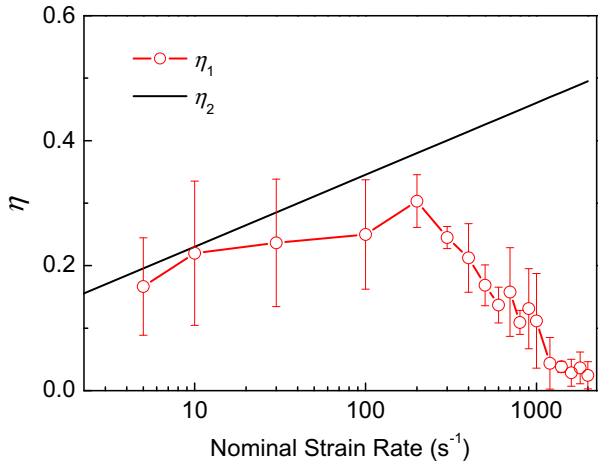

Fig. 10. Relative increase in the plateau stress of honeycombs made of material SR1 at different nominal strain-rates.

or influence on the plateau stress under both quasi-static and dynamic cases. The effect might be well submerged into experimental scatter for irregular cellular metals.

The variation of the relative increase in the plateau stress with the nominal strain-rates for honeycombs made of materials RS1 and RS2 is shown in Figs. 10 and 11, respectively. The relative increase in the plateau stress is always less than the relative increase in the flow stress of the corresponding solid material. It is found from Fig. 10 that the increase in the plateau stress due to the strain-rate sensitivity of cell wall material is getting smaller and smaller especially when the velocity is higher in our paper. About 20% increase in the plateau stress is found under the Quasi-static Homogeneous Mode when the strain rate is smaller than 400 s^{-1} for material RS1 used in this paper, as shown in Fig. 10. However, if the cell wall material is very sensitive to the strain rate, as material RS2, the increase of the plateau stresses is much bigger, Fig. 11. It is interesting to note that under the Transitional Mode and Shock Mode, the strain-rate effect seemingly decreases fast with the increase of impact velocity, in comparison with the inertia effect.

4. Discussion

4.1. Deformation mechanisms

The compressive stress–strain curves of the elastic–perfectly plastic honeycombs all show a linear-elastic regime followed by a plateau of roughly constant stress, and finally a densification regime with steeply rising stress. The deformation mechanism of the plateau regime was checked for honeycombs compressed under impact velocity $v = 1$ m/s. It is found that plastic hinges formed at the joints of cell walls in the shear band areas, but there are also some "S"-shaped walls nearby which are in elastic stress state, as shown in Fig. 12a and b. Plastic hinges are also found in the shear band areas for honeycombs of the other two kinds of cell wall material, but there are some differences. Not only plastic hinges but also plastic zones occur in the short cell walls of the bilinear material, as shown in Fig. 12c. For the strain-rate hardening material, some short cell walls become fully plastic, especially for material RS2.

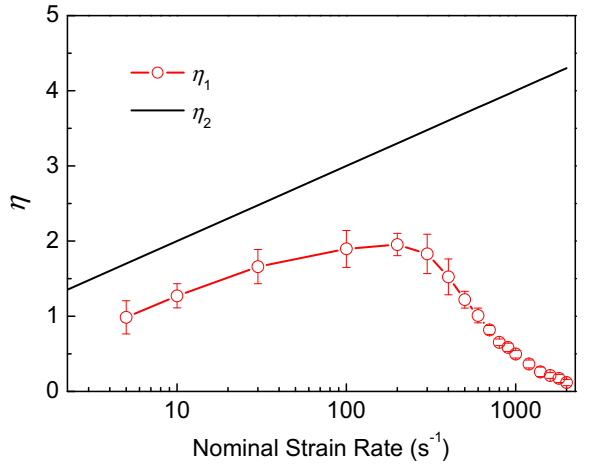

Fig. 11. Relative increase in the plateau stress of honeycombs made of material SR2 at different nominal strain-rates.

4.2. Shock front velocity

According to the definition of the Shock Mode given in Section 3.1, the distance between the impact end and the shock front Δs can be measured approximately, as shown in Fig. 2c. So the shock front propagation velocity V_S could be calculated as

$$V_S = V_0 + \Delta s/\Delta t \tag{15}$$

where V_0 is the impact velocity and Δt the corresponding time. For the impact velocities of 90 and 100 m/s, the evaluated shock front

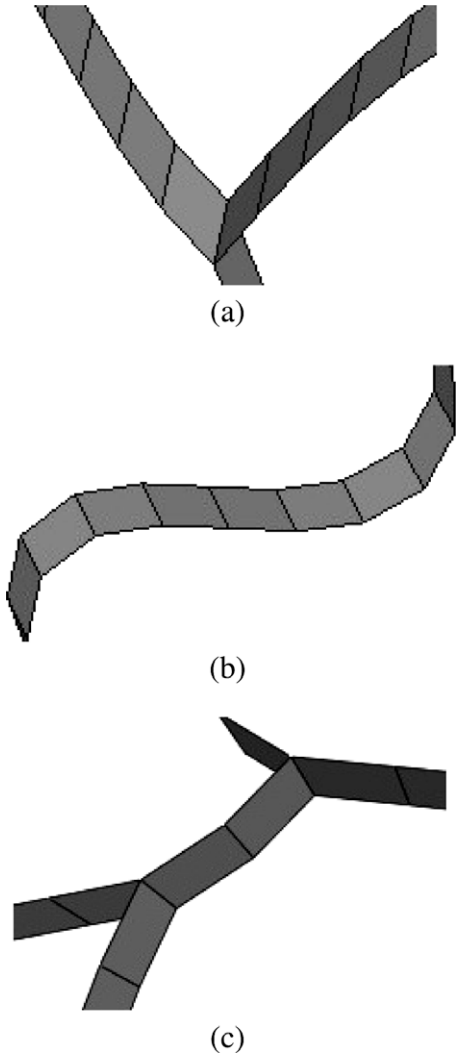

Fig. 12. Deformation of cell walls for honeycombs compressed under impact velocity $v = 1$ m/s: (a) plastic hinge at joint, (b) S-shaped cell walls and (c) plastic zone in short cell wall.

velocities are 105.3 and 118.4 m/s, respectively, as shown in Fig. 13. It is obvious that the shock front velocity increases as the impact velocity increases. Similar results were also obtained by Pattofatto et al. (2007).

According to Li and Reid (2006), the shock velocity can be expressed approximately as

$$V_S = \sqrt{\frac{1}{\rho_0}\frac{[\sigma]}{[\varepsilon]}} \tag{16}$$

where $[\sigma] = \sigma^i_{\mathrm{pl}} - \sigma^s_{\mathrm{pl}}$ and $[\varepsilon] = \varepsilon_D - \varepsilon_{cr} \approx \varepsilon_D$, and ρ_0 is the density of the honeycomb. Using this method, the calculated shock velocities are 113.3 and 124.7 m/s for the impact velocities of 90 and 100 m/s, respectively, which are a little larger than those calculated from the numerical simulation.

4.3. Energy

To explore the inertia effect and the strain-rate effect further, we performed energy analysis of the deformation of RS2 honeycomb. The energy balance is given by

$$E_I + E_{KE} - W = E_{total} = \text{constant}, \tag{17}$$

where E_I is the internal energy which mainly consists of elastic strain energy and plastic dissipation, E_{KE} is the kinetic energy and W the external work. The variations of elastic strain energy, plastic dissipation and kinetic energy with compressed length under impact velocities of 10, 100 and 180 m/s, corresponding to Homogeneous Mode, Transition Mode and Shock Mode for material RS2, are shown in Figs. 14–16, respectively.

It can be seen from Fig. 14 that under Quasi-static Homogeneous Mode, both the elastic strain energy and kinetic energy are much smaller than the plastic dissipation, indicating a negligible inertia effect. As the impact velocity increases, the kinetic energy increases significantly due to inertia effect while the elastic strain energy has little change, as shown in Figs. 15 and 16. It is also found that the plastic dissipation increases with the increasing impact velocity, which is caused by the enhanced plateau stress due to inertia effect.

4.4. Micro-inertia effect

According to the static load–distance curve, we could distinguish two energy absorbing structures: Type I and Type II (Lu and Yu, 2003). For a Type II structure under dynamic loading, the lateral inertia is much larger than the longitudinal (loading direction) inertia. Zhang and Yu (1989) established a simple crooked plate structure model based on classical inelastic collision theory. The collision system contained an impact rigid block and a pair of crooked plates. The equivalent mass of the crooked plate was expressed as

$$m_s = m + \frac{m}{3\sin^2\theta_0} \approx m + \frac{m}{3\theta_0^2}, \tag{18}$$

where m and θ_0 are the mass and the initial angle of the crooked plate, respectively. The first term and the second term on the right hand side of Eq. (18) stand for the longitudinal inertia and lateral inertia, respectively. θ_0 usually is small, so the lateral inertia is much lager than the longitudinal inertia. The ratio of the lateral and longitudinal inertia is important to understand the differences between Type I and Type II structure under dynamic loading. In our study, instead of using the equivalent mass to estimate this ratio, we will direct calculate the acceleration in lateral and longitudinal directions.

Generally speaking, the lateral inertia includes both translational and rotational inertia. However, in our simulation models, the rotational inertia is negligible. So, in order to estimate the micro-inertia effect (refers to the lateral inertia), we calculated the acceleration of all element nodes on one side of the honeycomb. The mean square root of the acceleration component is given by

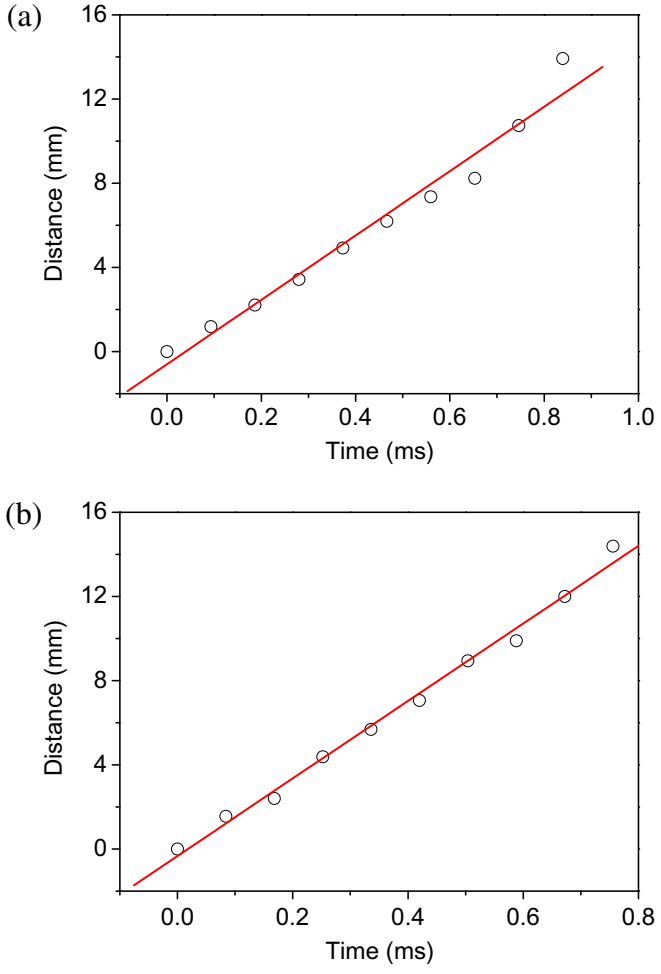

Fig. 13. Change of distance at different impact velocities of (a) $v = 90$ m/s, (b) $v = 100$ m/s.

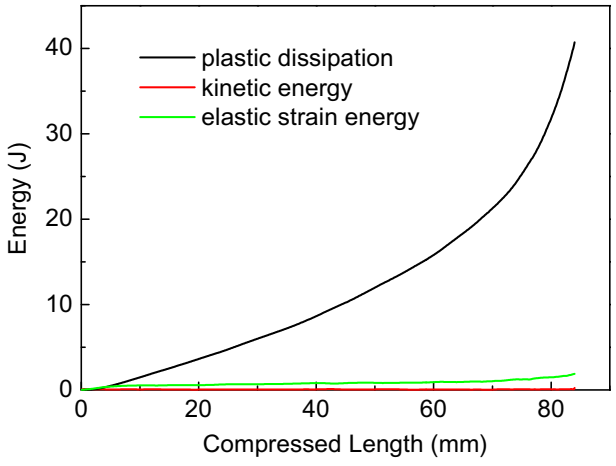

Fig. 14. Variations of elastic strain energy, plastic dissipation and kinetic energy with compressed length when the impact velocity is 10 m/s.

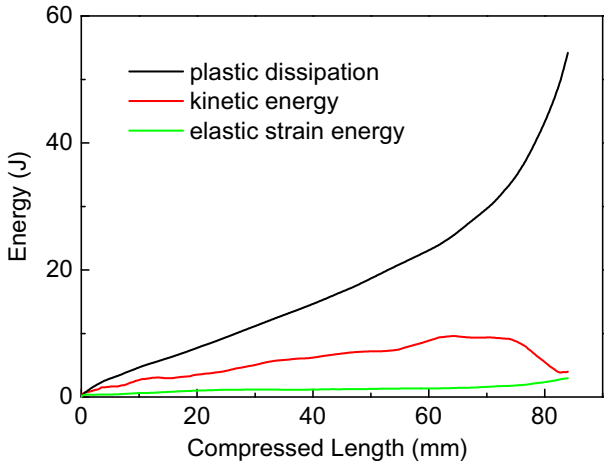

Fig. 15. Variations of elastic strain energy, plastic dissipation and kinetic energy with compressed length when the impact velocity is 100 m/s.

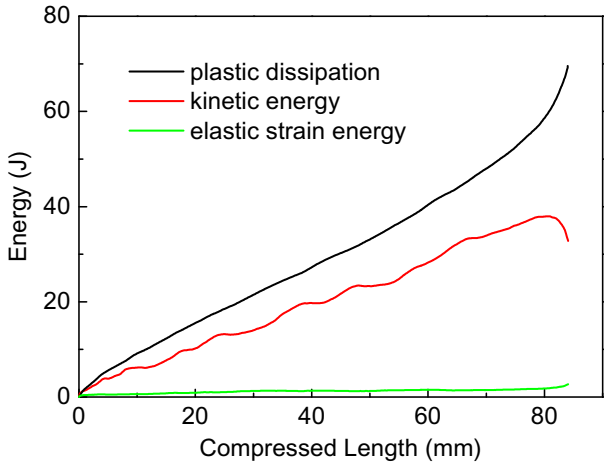

Fig. 16. Variations of elastic strain energy, plastic dissipation and kinetic energy with compressed length when the impact velocity is 180 m/s.

$$A = \left(\sum_{i=1}^{n} a_i^2 / n \right)^{1/2}, \tag{19}$$

where a_i is the acceleration of the ith node in x direction (loading direction) or y direction (transverse direction), n is the number of total nodes on one side of the honeycomb model.

To estimate the significance of the micro-inertia effect for the 2D random Voronoi honeycomb, we introduce the transverse-to-longitudinal acceleration ratio μ defined as

$$\mu = A_y / A_x, \tag{20}$$

where A_x and A_y are the mean square root of the accelerations in loading direction and transverse direction, respectively.

In the case of dense materials, the value of μ reflects the macroscopic transverse inertia effect. For a solid cylinder, if we neglect the wave propagation and assume a linear distribution of acceleration in longitudinal and radial directions, this ratio is

$$\mu = \sqrt{\frac{3}{2}} \frac{vR}{H}, \tag{21}$$

where R and H are the radius and height of the cylinder, respectively, v is the Poisson's ratio (in plastic case $v = .5$). Similarly, for a solid plate, we have

$$\mu = \frac{v}{2} \frac{B}{H}, \tag{22}$$

where B and H are the width and height of the plate, respectively.

In the case of cellular materials, the value of μ reflects both the macroscopic and microscopic transverse inertia effects. The variation of μ with the compressed length under different impact velocities for Voronoi honeycombs made from elastic–perfectly plastic material is shown in Fig. 17. It transpired that the value of μ is larger than that for a solid plastic square plate ($\mu = 0.25$ according to Eq. (21)), but much smaller than that for a typical Type II structure. It is interesting to notice that the value of μ decreases with the increase of impact velocity, indicating that the micro-inertia effect for the random Voronoi structure is relatively weak.

5. Conclusions

In this paper we have explored the effect of inertia and the properties of cell-wall materials on the rate sensitivity of Voronoi honeycombs. Three deformation modes, i.e., Homogeneous Mode, Transition Mode and Shock Mode, are found in different velocity ranges. The calculated nominal stress–strain curves in Homogeneous Mode are almost identical, regardless of the differences in impact velocity and density of cell wall material. This is in agreement with the discussion on the rate effect due to the intrinsic length scale presented in Section 1.

The deformation mechanisms, the dependence of plateau stress on the relative density, the energy distribution and the micro-inertia effect are also discussed. The micro-inertia effect is weak especially under high-velocity impact, in agreement with Tan et al. (2005a). Our present numerical results indicate that inertia is a dominant factor which affects the dynamic response of cellular metals. Due to this effect, the deformation becomes inhomogeneous and the plateau stress on the impact surface increases rapidly when the impact velocity exceeds a critical velocity, i.e., the transition velocity from Homogeneous Mode to Transition Mode. In this case the nominal stress–strain curve loses its physical meaning since it depends on the size of "specimen". The rate effect of the Voronoi honeycombs exhibited under high-velocity impact is an inertia effect, rather than the strain-rate effect.

In comparison with the inertia effect, the strain hardening of cell-wall material contributes a little and the strain-rate sensitivity of cell-wall material leads to an increase in plateau stress but it cannot explain the strong rate dependence observed in some metallic foams. More elaborate experiments and punctilious analysis are required to solve the existing puzzle thoroughly.

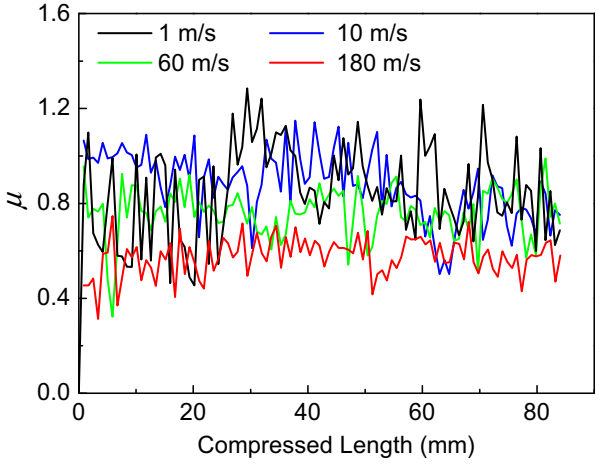

Fig. 17. Comparison of parameter μ under different impact velocities.

Some possible mechanisms responsible to the rate sensitivity of metallic foams need to be further explored, e.g., cell morphology, cell wall material distribution, ductile–brittle transition of the cell wall material, strain-rate sensitivity of its failure strain, and microstructural characters associated with their manufacture. These factors may result in different deformation modes under quasi-static and dynamic loads.

Acknowledgements

The work reported herein is supported by the National Natural Science Foundation of China (Projects Nos. 10532020, 10672156 and 90205003).

References

Dannemann, K.A., Lankford, J., 2000. High strain rate compression of closed-cell aluminium foams. Materials Science and Engineering A 293, 157–164.

Deshpande, V.S., Fleck, N.A., 2000. High strain rate compressive behaviour of aluminium alloy foams. International Journal of Impact Engineering 24, 277–298.

Gibson, L.J., Ashby, M.F., 1997. Cellular Solids: Structure and Properties, second ed. Cambridge University Press, Cambridge, MA.

Hall, I.W., Guden, M., Yu, C.J., 2000. Crushing of aluminum closed cell foams: density and strain rate effects. Scripta Materialia 43, 515–521.

Han, F.S., Cheng, H.F., Li, Z.B., Wang, Q., 2005. The strain rate effect of an open cell aluminum foam. Metallurgical and Materials Transactions A 36, 645–650.

Harrigan, J.J., Reid, S.R., Peng, C., 1999. Inertia effects in impact energy absorbing materials and structures. International Journal of Impact Engineering 22, 955–979.

Harrigan, J.J., Reid, S.R., Tan, P.J., Reddy, T.Y., 2005. High rate crushing of wood along the grain. International Journal of Mechanical Sciences 47, 521–544.

Johnson, G.R., Cook, W.H., 1983. A constitutive model and data for metals subjected to large strains, high strain rates and high temperatures. In: Proceedings of the Seventh International Symposium on Ballistics, The Hague, Netherlands, pp. 541–547.

Kanahashi, H., Mukai, T., Yamada, Y., Shimijima, K., Mabuchi, M., Nieh, T.G., Higashi, K., 2000. Dynamic compression of an ultra-low density aluminium foam. Materials Science and Engineering A 280, 349–353.

Lee, S., Barthelat, F., Moldovan, N., Espinosa, H.D., 2006. Deformation rate effects on failure modes of open-cell Al foams and textile cellular materials. International Journal of Solids and Structures 43, 53–73.

Li, Q.M., Reid, S.R., 2006. About one-dimensional shock propagation in a cellular material. International Journal of Impact and Engineering 32, 1898–1906.

Li, K., Gao, X.L., Wang, J., 2007. Dynamic crushing behavior of honeycomb structures with irregular cell shapes and non-uniform cell wall thickness. International Journal of Solids and Structures 44, 5003–5026.

Lu, G.X., Yu, T.X., 2003. Energy Absorption of Structures and Materials. Woodhead, Cambridge.

Ma, G.W., Ye, Z.Q., Shao, Z.S., 2009. Modeling loading rate effect on crushing stress of metallic cellular materials. International Journal of Impact Engineering 36, 775–782.

Montanini, R., 2005. Measurement of strain rate sensitivity of aluminium foams for energy dissipation. International Journal of Mechanical Sciences 47, 26–42.

Mukai, T., Miyoshi, T., Nakano, S., Somekawa, H., Higashi, K., 2006. Compressive response of a closed-cell aluminum foam at high strain rate. Scripta Materialia 54, 533–537.

Pattofatto, S., Elnasri, I., Zhao, H., Tsitsiris, H., Hild, F., Girard, Y., 2007. Shock enhancement of cellular structures under impact loading: part II analysis. Journal of the Mechanics and Physics of Solids 55, 2672–2686.

Paul, A., Ramamutry, U., 2000. Strain rate sensitivity of a closed-cell aluminum foam. Materials Science and Engineering A 281, 1–7.

Reid, S.R., Peng, C., 1997. Dynamic uniaxial crushing of wood. International Journal of Impact Engineering 19, 531–570.

Ruan, D., Lu, G., Wang, B., Yu, T.X., 2003. In-plane dynamic crushing of honeycombs – a finite element study. International Journal of Impact Engineering 28, 161–182.

Silva, M.J., Hayes, W.C., Gibson, L.J., 1995. The effects of non-periodic microstructure on the elastic properties of two-dimensional cellular solids. International Journal of Mechanical Sciences 37, 1161–1177.

Tan, P.J., Reid, S.R., Harrigan, J.J., Zou, Z., Li, S., 2005a. Dynamic compressive strength properties of aluminium foams. Part I – experimental data and observations. Journal of the Mechanics and Physics of Solids 53, 2174–2205.

Tan, P.J., Reid, S.R., Harrigan, J.J., Zou, Z., Li, S., 2005b. Dynamic compressive strength properties of aluminium foams. Part II – 'shock' theory and comparison with experimental data and numerical models. Journal of the Mechanics and Physics of Solids 53, 2206–2230.

Tekoglu, C., Onck, P.R., 2005. Size effects in the mechanical behavior of cellular materials. Journal of Materials Science 40, 5911–5917.

Tekoglu, C., Onck, P.R., 2008. Size effects in two-dimensional Voronoi foams: a comparison between generalized continua and discrete models. Journal of the Mechanics and Physics of Solids 56, 3541–3564.

Wang, Z.H., Ma, H.W., Zhao, L.M., Yang, G.T., 2006. Studies on the dynamic compressive properties of open-cell aluminum alloy foams. Scripta Materialia 54, 83–87.

Zhang, T.G., Yu, T.X., 1989. A note on a 'velocity sensitive' energy-absorbing structure. International Journal of Impact Engineering 8, 43–51.

Zhao, H., Abdennadher, S., 2004. On the strength enhancement under impact loading of square tubes made from rate insensitive metals. International Journal of Solids and Structures 41, 6677–6697.

Zhao, H., Elnasri, I., Abdennadher, S., 2005. An experimental study on the behaviour under impact loading of metallic cellular materials. International Journal of Mechanical Sciences 47, 757–774.

Zheng, Z.J., Yu, J.L., Li, J.R., 2005. Dynamic crushing of 2D cellular structures: a finite element study. International Journal of Impact Engineering 32, 650–664.

Zhu, H.X., Hobdell, J.R., Windle, A.H., 2001. Effects of cell irregularity on the elastic properties of 2D Voronoi honeycombs. Journal of the Mechanics and Physics of Solids 49, 857–870.

Zou, Z., Reid, S.R., Tan, P.J., Li, S., Harrigan, J.J., 2009. Dynamic crushing of honeycombs and features of shock fronts. International Journal of Impact Engineering 36, 165–176.